UDC 621.373.8: 621.375.826: 621.391.6

Cavity Length Dependence of Wavelength Conversion Efficiency of Four-wave Mixing in λ/4-shifted DFB Laser

●Takasi Simoyama ●Haruhiko Kuwatsuka ●Hiroshi Ishikawa

(Manuscript received June 17,1998)

Non-degenerate four-wave mixing in a semiconductor DFB laser using its lasing wave as pump waves is a promising method of attaining wide-range and high-bit-rate wavelength conversion in a single device. The structure dependence of the wavelength conversion efficiency in a lasing λ/4-shifted DFB laser has been analyzed for the first time. Systematic calculation of the optical field profile in DFB lasers has shown that a structure with a small grating coupling coefficient κ and a large cavity length *L* is a hopeful candidate for obtaining a high conversion efficiency. Experiments showed good agreements with the analytical results. For a structure of κ = 11 cm^{-1} and *L* = 1,300 μm, a very high conversion efficiency of –5 dB and extremely low noise characteristics at a large detuning of 1.6 THz have been attained.

1. Introduction

A wide-range wavelength converter will be required for the wavelength division multiplexed (WDM) optical communication systems of the near future. Wavelength conversion using non-degenerate four-wave-mixing (NDFWM) has been studied extensively because of its potential for realizing wide-range and high-bit-rate wavelength conversion. The NDFWM process can convert frequency modulated signals as well as amplitude modulated signals. NDFWM can also be used as the fiber dispersion compensater in long-distance transmission systems[1] because this process provides a conjugate, i.e., time reversal output of the input.

NDFWM in carrier injected semiconductor materials is an attractive candidate for attaining a high conversion efficiency with a small device (~1 mm) because of its large nonlinear susceptibility (over 1×10^{-16}m^2/V^2)[2] and linear gain, which amplifies not only converted waves but also input waves.

There are two possible devices that can take full advantage of these materials: semiconductor optical amplifiers (SOAs) and semiconductor lasers. From the viewpoint of the conversion efficiency, NDFWM in SOAs has already been studied extensively and a conversion efficiency of more than 0 dB has been accomplished,[3)-5)] while the laser structure is not yet optimized for the NDFWM processes. NDFWM in a semiconductor laser, compared to NDFWM in an SOA, has the great advantage of practicality. In the case of the laser, the pump wave is provided by the laser itself, so there is no need to prepare an external pump wave source. Thus, a wavelength converter consisting of a single device is readily obtained. To make these devices really applicable, however, they must achieve a much higher conversion efficiency. This paper presents guidelines for optimizing the laser structure for NDFWM processes. The guidelines are based on theoretical analysis and experimental results and are designed to optimize the conversion efficiency to noise ratio rather than the efficiency itself.

This paper is organized as follows. In Chap-

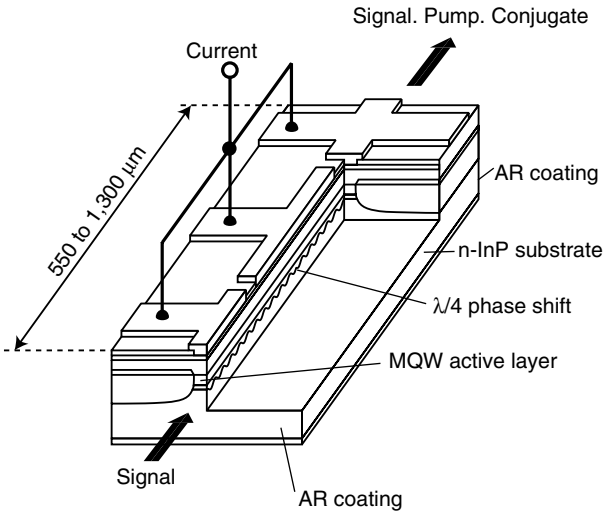

Figure 1
λ/4-phase-shifted DFB laser with AR coated facets.

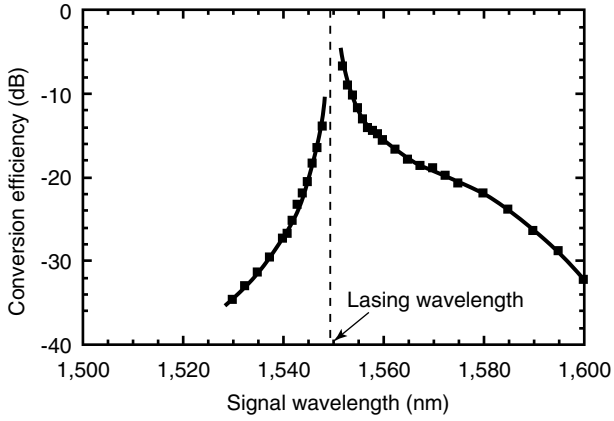

Figure 2
Signal wavelength dependence of conversion efficiency.

ter 2, the features of the NDFWM in a λ/4 -shifted DFB laser and the kind of characteristics required for this device are explained. In Chapter 3, analytic results are shown. The calculation method used to estimate the conversion efficiency and the noise level is explained, and the laser structure dependencies of the conversion efficiency to noise ratio are discussed. Chapter 4 describes experiments that were done to check the validity of the analysis. The experimental results of the conversion efficiency versus cavity length are shown, and the results are compared to the analysis. Chapter 5 compares these results with a typical report of NDFWM in an SOA.

2. Four-wave mixing in λ/4 -shifted DFB laser

A λ/4-phase-shifted distributed feedback (DFB) laser with anti-reflection (AR) coating on both facets (**Figure 1**) is the most appropriate choice for single device operation of the NDFWM process.[6),7)] Stable lasing waves working as pump waves could be generated in the middle of the stop band, as opposed to the uniform corrugation DFB lasers, which require another master laser for stabilizing the pump.[8)] The DFB laser also works as an SOA for input signal waves or output conjugate waves whose wavelengths lie outside the stop band. As a result, conversion efficiency is not affected by sharp Fabry-Perot resonances, and a wide range of wavelength signals can be converted.

Using this device as a single device operated wavelength converter, some fundamental experiments have already been performed.[7)] In these experiments, a device with a grating coupling coefficient of 12.2 cm^{-1} and a cavity length of 900 μm was used. A relatively high conversion efficiency of –6 dB at 1.75 nm (220 GHz) detuning between the pump and the signal was obtained. The detuning dependence of the conversion efficiency was measured, and wavelength conversion over a range of more than 60 nm was reported (**Figure 2**). The third order optical nonlinear susceptibility $\chi^{(3)}$ was estimated, and it was clear that the value of $\chi^{(3)}$ was determined by the sum of nonlinear effects such as the carrier modulation effect, carrier heating effect, and spectral hole burning effect. Also, the saturation characteristics were investigated and a maximum conjugate power of –7.3 dBm was obtained at an input signal power of 2.2 dBm. In terms of the noise characteristics, a conjugate output to noise ratio of 37 dB was demonstrated at an input of 0 dBm and a detuning of 2.5 nm. These results are, for fundamental research, fairly good and promising. How-

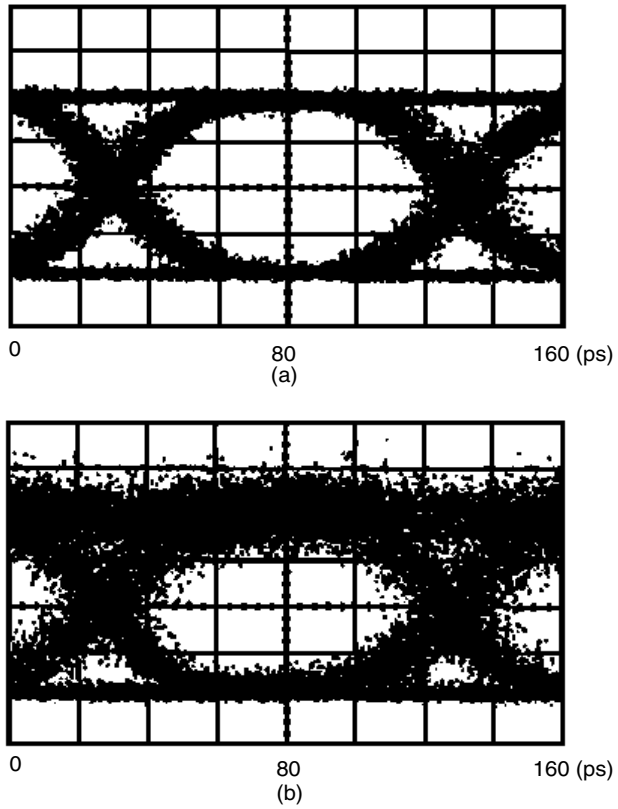

Figure 3
Eye patterns of 10 Gbit/s NRZ signal: (a) Before transmission (b) After transmission.

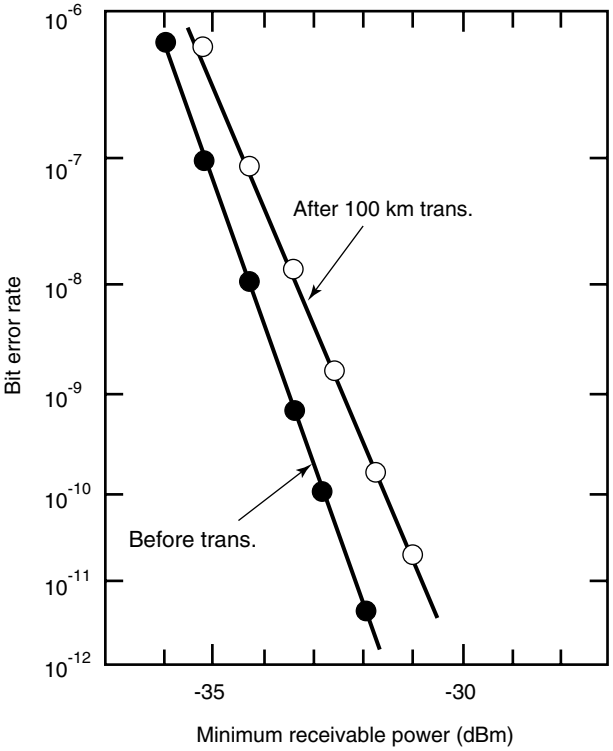

Figure 4
Bit error rate of 10 Gbit/s NRZ signal.

ever, for a practical wavelength converter, they are not sufficient, especially in terms of the conversion efficiency.

Also, a preliminary experiment demonstrating fiber dispersion compensation was performed using this device.[1] The outline of the experiment is as follows. A 10 Gb/s NRZ signal was introduced into a single mode optical fiber (SMF). After 50 km of transmission, the signal was converted into the conjugate by FWM in the λ/4-shifted DFB laser and then amplified by an erbium doped fiber amplifier (EDFA). The converted signal was retransmitted for another 50 km in SMF; thus, a total of 100 km of optical transmission was completed. The waveform was observed before and after the 100 km transmission. The eye patterns of these transmissions are shown in **Figure 3**. After 50 km of transmission, the waveform is distorted due to finite chromatic dispersion. But after an additional 50 km (total 100 km), the conjugate wave is inversely affected by the chromatic dispersion and the eye pattern is restored [Figure 3(b)]. The result confirms that NDFWM in the DFB laser can be used for dispersion compensation.

However, the eye pattern after 100 km is somewhat noisy. **Figure 4** shows the bit error rate (BER) characteristics before and after transmission. The power penalty of 2 dB is observed at a 10^{-11} BER level. This is due to the noise from the amplified spontaneous emission (ASE) in the laser. In carrier injected materials, the generation of ASE noise is an intrinsic problem. Thus, a laser structure which has both a high conversion efficiency and a low ASE level is required.

The conversion efficiency of NDFWM in SOAs or lasers is decided by (1) the absolute value of the third order non-linear susceptibility $\chi^{(3)}$, (2) the intensity of pump waves, (3) the intensity of input signal waves, (4) the linear gain which

amplifies input signal waves or output conjugate waves, and (5) the length for non-linear interaction between pump waves and input signal waves. Among those factors, (4) and (5) are obtained differently in SOAs than in lasers. In SOAs, a larger interaction length and a higher linear gain can be obtained simultaneously by lengthening the device, which also improves the conversion efficiency. But, this is not the case with NDFWM in lasers. The linear gain in the laser is clamped at the threshold gain, and the threshold gain is inversely proportional to the cavity length. Consequently, in the case of lasers, it is not obvious which structure is optimal for a good conversion efficiency.

Although a large linear gain increases the conversion efficiency, it also increases the ASE level. In the case of an SOA, it is well known that high-power saturated operation with a long device can suppress the ASE. It is also necessary, therefore, to consider the ASE in the case of lasers.

3. Theoretical analysis of conversion efficiency

3.1 Assumption for analysis

The authors made the following assumptions in the analysis to abstract the essence of the NDFWM process:

1) The phase-matching condition between signal and pump waves propagating in the same direction is satisfied inside the entire cavity. The coherent length for phase matching is 1.8 mm, even in the case of the large wavelength detuning of 40 nm when the pump wavelength is near 1.55 μm. In this paper, laser structures whose cavity length is less than 1.5 mm are considered, thus, this assumption is valid.
2) The signal and the conjugate waves outside the stop band are not affected by the grating in the DFB laser waveguide, i.e., the laser works as though it is a traveling wave SOA for these waves.
3) The pump and the signal optical field profile are not affected by the pump-signal nonlinear interaction. Under the experimental conditions described later, the amplified signal output is –15 dB smaller than the pump output. The interaction is three orders of magnitude smaller than the linear gain and could be negligible.
4) The third-order optical nonlinear susceptibility $\chi^{(3)}$ was assumed to be constant along the propagation direction in the cavity. It is the carrier density profile that makes the largest contribution to the profile of $\chi^{(3)}$. We considered only the case of uniform current injection in the entire cavity, so the carrier density, which is decided by the quasi-fermi-level, is approximately uniform.

3.2 Calculation of optical field profile in DFB lasers

From the above assumptions, we can obtain the profiles of the pump wave and signal wave independently. Then, the conjugate wave can be calculated in a straight forward fashion.

The electric field profile of the pump wave in the longitudinal direction evolves according to Maxwell's wave-equation. In the grating waveguide, the whole electric field is described as the sum of a pair of waves traveling in opposite directions[9]:

$$E_p(z)=R(z)\exp(-i\beta_0 z)+S(z)\exp(i\beta_0 z), \quad (1)$$

where the z axis is the optical axis in the laser with $z = 0$ at one end and $z = L$ (L : cavity length) at the other end, Ep is the electric field of the pump waves without the time evolution terms, R (S) is the envelope function of the optical wave propagating in the positive (negative) z-direction, and β_0 is the wavenumber of the corrugation. Maxwell's equation and Equation (1) reduce to the coupled mode wave equations for R and S as follows:

$$-\frac{dR}{dz}+\left[\frac{g_p}{2}-j(\beta-\beta_0)\right]R = j\kappa e^{-j\Omega}S \quad (2)$$

$$\frac{dS}{dz} + \left[\frac{g_p}{2} - j(ß - ß_0)\right]S = j\kappa e^{j\Omega}R, \qquad (3)$$

where g_p is the linear gain, ß is the wavenumber of the lasing wavelength, κ is the coupling coefficient of the corrugation, and Ω is the phase shift of the corrugation; which is equal to π for the λ/4-shifted DFB laser. Equations (2) and (3) can be solved under the conditions that R (S) is equal to zero at the $z = 0$ ($z = L$) position and R and S are continuous at the phase shift position. The threshold gain g_{th} is also calculated at the same time.

The signal wave evolves as in an SOA:

$$\frac{dE_s}{dz} = \frac{\Gamma g(\omega_s)}{2} E_s, \qquad (4)$$

where Γ is the optical confinement factor for the active layer in the waveguide.

From the assumptions given in the previous subsection, the development of the conjugate wave is given as:

$$\frac{dE_i}{dz} = \Gamma\left[\frac{g(\omega_i)}{2} E_i + i\frac{3\mu_0\varepsilon_0\omega_i^2}{8k_i}\chi^{(3)}(\omega_i;\omega_p,\omega_p,-\omega_s)R^2E_s\right], \qquad (5)$$

where $\chi^{(3)}$ is the third-order optical nonlinear susceptibility.

Figure 5 shows the development of the pump, the signal, and the conjugate wave obtained from the above equations. Three cases are shown: case (a): $\kappa L = 0.65$, case (b): $\kappa L = 1.43$, and case (c): $\kappa L = 3.90$. These figures tell us useful information about the NDFWM processes in the laser. As the parameter κL becomes larger, the pump wave's profile becomes more concentrated at the center of the cavity, and, because of the smaller threshold gain, the signal wave's growth becomes slower. As a result, for a large κL cavity the conjugate wave's growth position is shifted to the center of the waveguide.

We need to know the ASE level for the signal to noise ratio (SNR) at the conjugate wave's frequency. We can calculate the ASE intensity I_{ASE} from the following equation[10]:

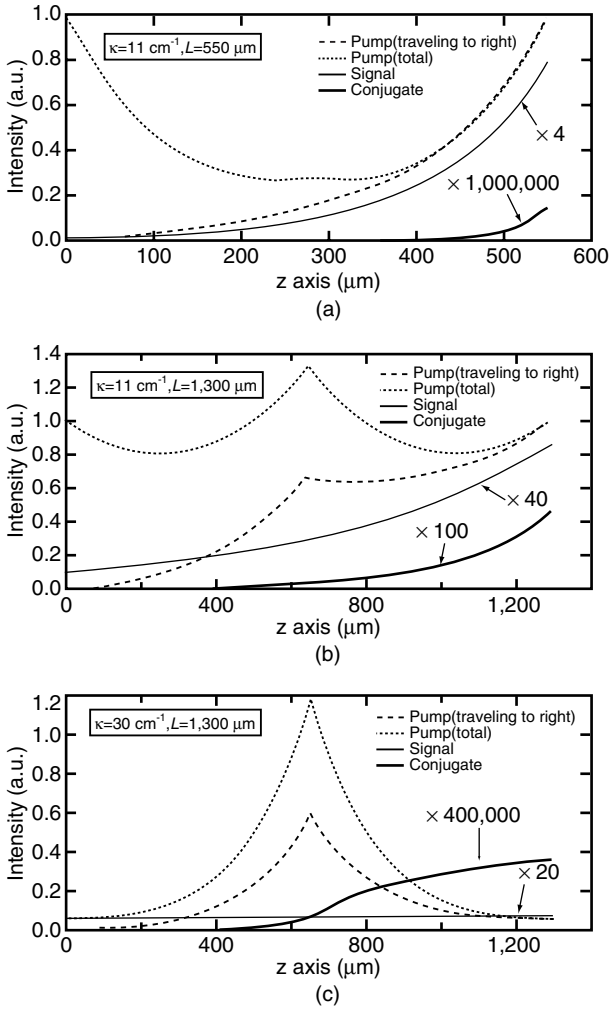

Figure 5
Calculated optical intensity profiles in DFB laser: (a) κL=0.65, (b) κL=1.43, (c) κL=3.90.

$$\frac{dI_{ASE}}{dz} = \Gamma g I_{ASE} + \frac{Crh\omega}{4\pi}, \qquad (6)$$

where C is the fraction of spontaneous emission coupled into the guide mode, g is the net gain, and r is the radiative recombination rate.

3.3 Dependence of conversion efficiency on the laser structure

From the method described above, some characteristics, i.e., the threshold gain, wavelength conversion efficiency, and noise level, can be calculated. Systematic calculation of these quantities reveals the structural dependence of these characteristics.

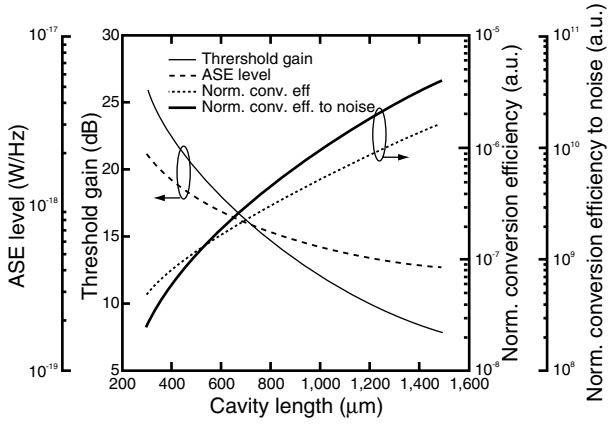

Figure 6
Cavity length dependence of conversion efficiency.

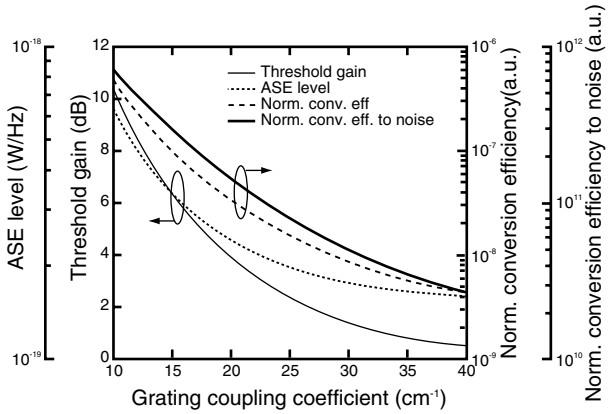

Figure 7
Grating coupling coefficient dependence of conversion efficiency.

Figure 6 shows the cavity length dependence of several characteristics when the grating coupling coefficient κ is taken to be the relatively small value of 11 cm^{-1}. The threshold gain, ASE level, normalized conversion efficiency, and normalized conversion efficiency to noise ratio are plotted. Normalization was done based on the square of the maximum pump power along the z axis to eliminate the effect of differences in pump power.

From the figure, we can see that the normalized conversion efficiency increases as the cavity is lengthened, while the threshold gain becomes smaller. This means that, for structures with a small κ coefficient, when the interaction length is made large, the beneficial effect on the conversion efficiency outweighs the negative effects that are due to the smaller linear gain. In addition, in contrast to the case in SOAs, the ASE level is lower for a longer cavity length. As a result, the conversion efficiency to noise ratio, which is the most important characteristic of a wavelength converter, becomes very high in a longer cavity device; for example, increasing the length from 550 μm to 1,300 μm improves the ratio by 13 dB.

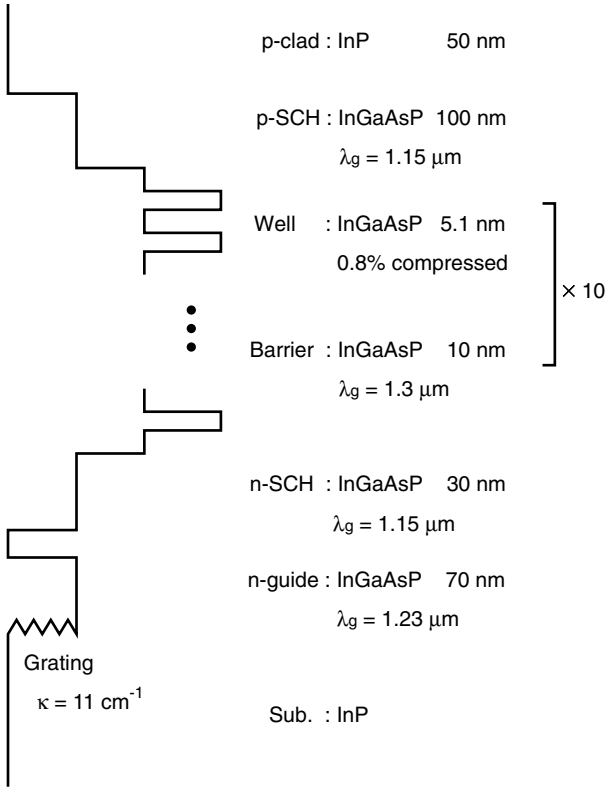

Figure 8
Layer structure of laser.

Next, **Figure 7** shows the κ coefficient dependence of the characteristics when the cavity is taken to the relatively long length of 1,300 μm. This figure shows that a small κ structure is advantageous in terms of these characteristics. This is because the concentration of the pump wave profile at the cavity center results in the suppression of total nonlinear interaction between the pump and the signal and also because the linear gain is reduced.

4. Experimental results

4.1 Experimental setup

Based on the findings described in the previous chapter, we fabricated λ/4-phase-shifted DFB lasers with a small κ and various cavity lengths. The wavelength conversion efficiencies and noise ratios were evaluated for these devices.

Figure 8 shows the layer structure of the devices. The active layer is a multiple quantum well (MQW) having 10 InGaAsP 0.8% compressive quantum well layers and a photoluminescence spectrum with a center wavelength of 1.565 μm. The corrugation was made on an InP substrate, and a separate optical guide layer was made directly on the substrate. Figure 8 also shows various other information, for example, the width and band gap wavelength of each layer. The optical confinement to the active layers is estimated to be 10%, and the coupling coefficient to the grating is estimated to be 11 cm^{-1}. We fabricated the semi-insulated planar buried hetero (SI-PBH) structure shown in Figure 1. The cleaved facets are anti-reflection-coated by the TiON/MgF bilayer. Samples with cavity lengths of 550, 800, 1,050, 1,300 μm were made.

The measurement was performed as follows. A uniform current of 100 mA /300 μm was injected into all of the samples except the 1,300 μm samples. The 1,300 μm samples were operated at 70 mA/300 μm because they exhibited multimode lasing at a large injection current. The temperature was held at 15°C. The lasing wavelengths were 1.48 to 1.51 μm , and the threshold currents were about 10 mA for the 550 μm samples and about 20 mA for the 1,300 μm samples. Input signal waves from a variable wavelength light source were polarization-controlled to maximize the conversion efficiency and coupled into one side facet of the laser. The input wave power was typically 40 to 100 μW. The dependence of the conversion efficiency on the input power was negligible because saturation did not occur at this range of power. The input wave's wavelength was adjusted to 5, 10, or 20 Trad/s (0.8, 1.6, or 3.2 THz) detunings from the lasing pump wave. Output waves consisting of the pump, signal, and conjugate waves from the other side of the facet were observed with an optical spectrum analyzer, and the conversion efficiencies were estimated for each detuning.

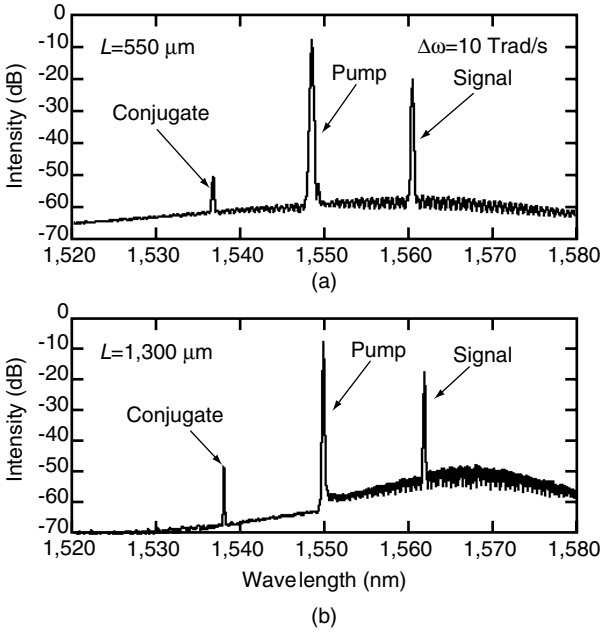

Figure 9
Spectra of NDFWM in DFB lasers: (a) *L*=550 μm, (b) *L*=1,300 μm

4.2 Dependence of conversion efficiency on the cavity length

Figure 9 shows typical measured spectra for 550 μm and 1,300 μm samples. The figures are for 10 Trad/s detuning between the input signal and the pump. Comparing these two figures, the ratio of conjugate wave intensity to ASE level is obviously higher in the longer cavity sample. A periodic resonant structure was also seen in these spectra for wavelengths longer than the pump wavelength. The periods are equal to the free spectral range (FSR) of the laser cavities, so these samples have a Fabry-Perot resonant structure due to the residual reflection from the AR coated facets. With a small κ, these devices are easily influenced by even a small amount of reflectance. To eliminate the effect of this resonant structure,

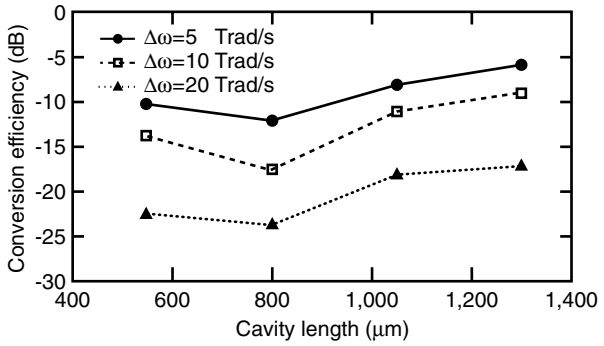

Figure 10
Experimental results of conversion efficiency for different cavity lengths.

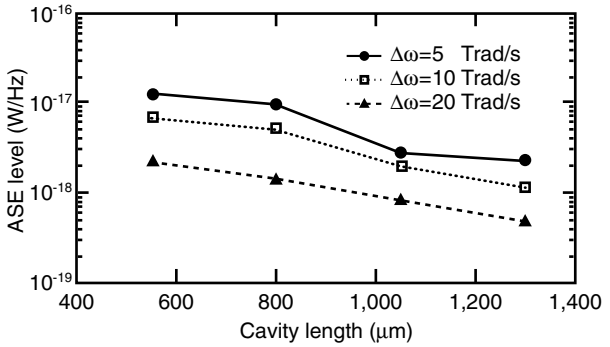

Figure 11
Experimental results of ASE level for different cavity lengths.

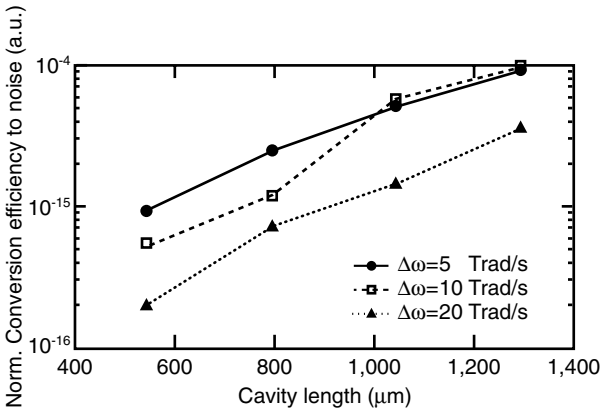

Figure 12
Experimental results of conversion efficiency to noise ratio for different cavity lengths.

measurements were performed for several signal waves of slightly different wavelengths, then the efficiency was obtained by averaging the results of each measurement.

Figure 10 shows the cavity length dependence of the wavelength conversion efficiency for detunings between the pump and signal of 5, 10, and 20 Trad/s (0.8, 1.6, and 3.2 THz). Qualitative tendencies agreed with the analysis described in Chapter 3, i.e., the longer the cavity, the higher the efficiency. A very high conversion efficiency was observed for the 1,300 μm sample; that is, -5 dB at a 5 Trad/s detuning and -9 dB at a 10 Trad/s detuning. Compared to earlier results obtained for the κ = 12.2 cm^{-1} and L = 900 μm device described in Reference 7), the efficiency is 8 to 9 dB better.

The cavity length dependence of the ASE level is shown in **Figure 11**. Again, the results agree qualitatively with the analysis in Chapter 3, i.e., the longer the cavity, the lower the ASE level. The ASE of the 550 μm device is five times larger than that of the 1,300 μm device. Only a 3 dB change was expected from the analysis. The difference between the analysis and the experiment is due to the shift of the gain peak wavelength due to the different threshold current densities of the different cavity lengths.

From the above results, the conversion efficiency to noise (ASE) ratio was obtained. **Figure 12** shows the cavity length dependence of the normalized conversion efficiency to noise ratio. The figure shows that the ratio is exponentially improved as the cavity length is increased. From 550 μm to 1,300 μm, there is a 10 dB improvement. This value agrees with the value of 13 dB that was expected from the analysis and shows that the rather simplified model we used was valid. The figure also shows that the ratio is slightly higher for a 10 Trad/s detuning than for a 5 Trad/s detuning in long-cavity (over 1,000 μm) devices. This is due to the correlation between the peak gain and the signal wave's wavelength. That is, because a long-cavity device's peak gain is closer to the signal wave's wavelength, the linear gain is higher and consequently signal waves grow more rapidly.

5. Comparison with SOAs

We will now compare these devices with SOAs in respect to the conversion efficiency and noise ratio. A conversion efficiency of +6 dB has been reported for an SOA at a detuning of 1 THz.[5] Although the experimental result of -5 dB at a detuning of 0.8 THz for the 1,300 μm DFB laser is still inferior to the SOA, there is still some space for improvement. In the experiments, the laser was used with only a 21 mW pump wave. The reason for this limit was that at higher levels of carrier injection, single-mode operation broke down and Fabry-Perot resonant peaks began to lase. We could achieve a larger pump power by further optimizing the facet AR coating or by using the slanted facet technique commonly used for SOA devices. If the pump power is improved by 3 dB, the conversion efficiency may be improved by 6 dB and over 0 dB of conversion would be realized.

In terms of the conversion efficiency to noise ratio, our results are superior to those reported in Reference 5) and are some of the best results for NDFWM in a carrier injected semiconductor device. Reference 5) reports a conversion efficiency of about 0 dB and a conjugate/ASE ratio of 21.1 dB at a detuning of 1 THz and a bandwidth of 5.6 GHz for a pump power of -2.2 dBm and an input signal power of -18 dBm. This ASE level corresponds to 4.2×10^{-17} W/Hz, while our results for the 1,300 μm DFB laser are 2.1×10^{-18} W/Hz at a detuning of 0.8 THz and 1.0×10^{-18} W/Hz at a detuning of 1.6 THz. The conversion efficiency to ASE ratio in the SOA corresponds to 2.4×10^{16} Hz/W, while the results for the 1,300 μm DFB laser are 1.5×10^{17} Hz/W at a detuning of 0.8 THz and 1.6×10^{17} Hz/W at a detuning of 1.6 THz. Thus, the noise level of the DFB laser is 13 to 16 dB lower and the ratio is about 8 dB greater as compared to the SOA. These differences between the DFB laser and the SOA are due to the extremely low ASE noise level of the laser.

6. Summary

This paper is the first to report on the structural dependence of wavelength conversion efficiency when the NDFWM process is used in a DFB laser. Some practical assumptions were introduced to calculate the optical field profile in λ/4-shifted DFB lasers. Theoretical analysis based on a simplified model reveals that a structure with a small grating coupling coefficient κ and a long cavity length L can achieve a very high conversion efficiency. To examine the validity of this analytical result, DFB lasers with a small κ of 11 cm^{-1} and lengths of 550, 800, 1,050, and 1,300 μm were fabricated. The dependences of the conversion efficiency to noise ratio on the cavity length obtained from experiments showed good agreement with the analysis. For the samples with the longest cavity length (1,300 μm), a very high conversion efficiency of -5 dB at a wide detuning of 1.6 THz and an extremely low noise level of 10^{-19} to 10^{-18} W/Hz were observed.

These results show that a λ/4-shifted DFB laser is suitable as a single-device wavelength converter. The high conversion efficiency to noise ratio obtained from a laser with a long cavity and a small grating coupling coefficient meets the precondition for a high-bit-rate signal converter.

References

1) S. Watanabe, H. Kuwatsuka, S. Takeda, and H. Ishikawa: Polarisation-insensitive wavelength conversion and phase conjugation using bi-directional forward four-wave mixing in a lasing DFB-LD. *Electron. Lett.*, **33**, pp.316-317 (1997).

2) M. Yamada: Theoretical analysis of nonlinear optical phenomena taking into account the beating vibration of the electron density in semiconductors. *J. Appl. Phys.*, **66**, pp.81-89 (1989).

3) A. D'Ottavi, E. Iannone, A. Meccozi, S. Scotti, and P. Spano: 4.3 terahertz four-wave mixing spectroscopy of InGaAsP semiconductor

amplifiers. *Appl. Phys. Lett.*, **65**, pp.2633-2635 (1994).

4) J. Zhou, N. Park, K. J. Vahara, M. A. Newkrik, and B. I. Miller: Four-wave mixing wavelength conversion efficiency in semiconductor traveling-wave amplifiers measured to 65 nm of wavelength shift. *IEEE. Photon. Technol. Lett.*, **6**, pp.984-987 (1994).
5) A. D'Ottavi, F. Martelli, P. Spano, A. Mecozzi, S. Scotti, R. Dall'Ara, J. Eckner, and G. Guekos: Very high efficiency four-wave mixing in a single semiconductor traveling-wave amplifier. *Appl. Phys. Lett.*, **68**, pp.2186-2188 (1996).
6) H. Kuwatsuka, H. Shoji, M. Matsuda, and H. Ishikawa: THz frequency conversion using nondegenerate four-wave mixing in an InGaAsP multi quantum well laser. *Electron. Lett.*, **31**, 24, pp.2108-2110 (1995).
7) H. Kuwatsuka, H. Shoji, M. Matsuda, and H. Ishikawa: Nondegenerate four-wave mixing in a long-cavity λ/4 -shifted DFB laser using its lasing beam as pump beams. *IEEE J. Quantum Electron.*, **33**, 11, pp.2002-2010 (1997).
8) E. Cerboneschi, D.Hennequin, and E. Arimondo: Frequency conversion in external cavity semiconductor lasers exposed to optical injection. *IEEE J. Quantum. Electon*, **29**, pp.1477-1487 (1996).
9) S. Akiba, M. Usami, and K. Utaka: 1.5- μmλ/4-shifted InGaAsP/InP DFB lasers. *J. Lightwave Technol.*, **LT-5**, pp.1564-1573 (1987).
10) M. J. Adams, J. V. Collins, and I. D. Henning: Analysis of semiconductor laser optical amplifiers. *in Inst. Elec. Eng.*, **132**, pp.58-63 (1985).

Takasi Simoyama received the B.S. and M.S. degrees in Applied Physics from the University of Tokyo, Japan in 1993 and 1995, respectively. He joined Fujitsu Laboratories Ltd., Atsugi in 1995, where he has been engaged in the research of optical semiconductor devices for optical communication systems. He is a member of the Japan Society of Applied Physics (JSPA).

Haruhiko Kuwatsuka received the B.S. and Dr. degrees in Applied Physics from the University of Tokyo, Japan in 1985 and 1993, respectively. He joined Fujitsu Laboratories Ltd., Atsugi in 1985, where he has been engaged in the research of optical semiconductor devices for optical communication systems. He is a member of the Japan Society of Applied Physics (JSPA) and the Institute of Electronics, Information and Communication Engineers (IEICE) of Japan.

Hiroshi Ishikawa received the B.S. and M.E. degrees in Electronics from the Tokyo Institute of Technology, Tokyo, Japan in 1970 and 1972, respectively. He joined Fujitsu Laboratories Ltd., Kawasaki in 1972, where he has been engaged in the research and development of semiconductor lasers for optical communications. He received the Dr. degree from the Tokyo Institute of Technology in 1984. He is a member of the Institute of Electronics, Information and Communication Engineers (IEICE) of Japan, the Japan Society of Applied Physics, and the Optical Society of America. Also, he is a senior member of the Institute of Electrical and Electronics Engineers (IEEE). He received the Young Engineers Award from the IEICE in 1976 and the Invention Prize for Encouragement from the Japan Institute of Invention and Innovation in 1990.